ADVANCED FUNCTIONAL MATERIALS

Supporting Information

for *Adv. Funct. Mater.*, DOI: 10.1002/adfm.201805105

Super Charge Separation and High Voltage Phase in Na_xMnO_2

*Xi Chen, Yichao Wang, Kamila Wiaderek, Xiahan Sang, Olaf Borkiewicz, Karena Chapman, James LeBeau, Jeffrey Lynn, and Xin Li**

Supporting Information

Super charge separation and high voltage phase in Na_xMnO_2

Xi Chen, Yichao Wang, Kamila Wiaderek, Xiahan Sang, Olaf Borkiewicz, Karena Chapman, James LeBeau, Jeffrey Lynn and Xin Li*

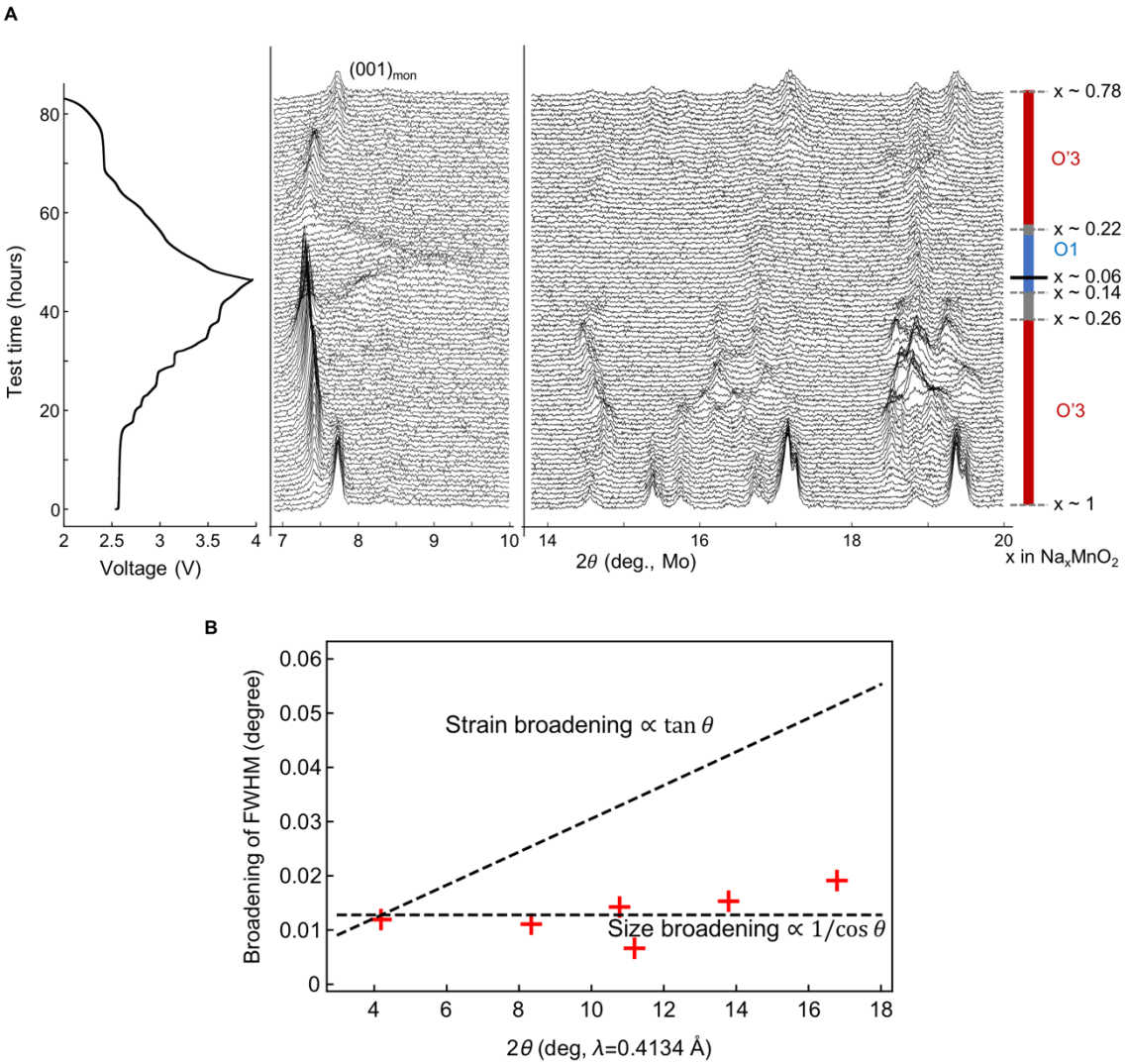

Figure S1 | *In-situ* lab XRD measurement of the first cycle of $NaMnO_2$. (**A**), Left panel: Voltage curve of the $NaMnO_2$ *in-situ* cell of the first cycle at C/50 rate, from 2V to 4V. Middle and right panel: *In-situ* XRD profiles collected with Mo source ($K_{\alpha 1}$ wavelength: 0.7093 Å) and the corresponding phase evolution. The O'3-O1 phase evolution is very close to the evolution identified from the *in-situ* SXRD cell. (**B**), Strain versus size broadening analysis. Red markers are the broadening of a series of peaks from O'3 to O1 in SXRD measurement (Fig.

2 in Main Text). Dashed lines stand for the angle dependence of size broadening and strain broadening.

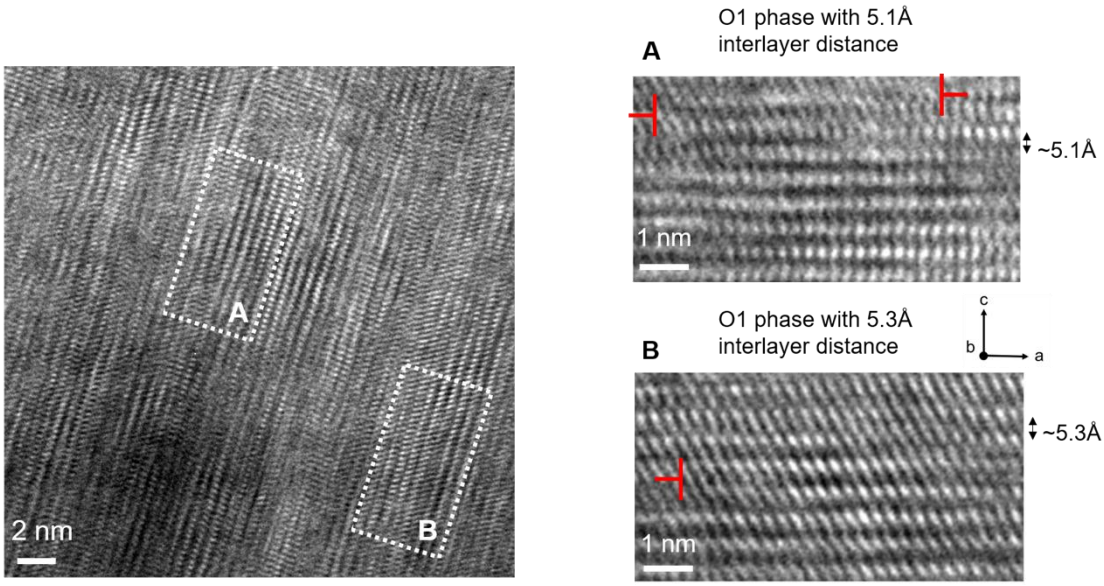

Figure S2 | HRTEM images of $NaMnO_2$ charged to 4.0V taken in *b* direction. O1 phase with interlayer distance around 5.1 Å (**A**) and 5.3 Å (**B**). Defects (marked with red) can be found in the images.

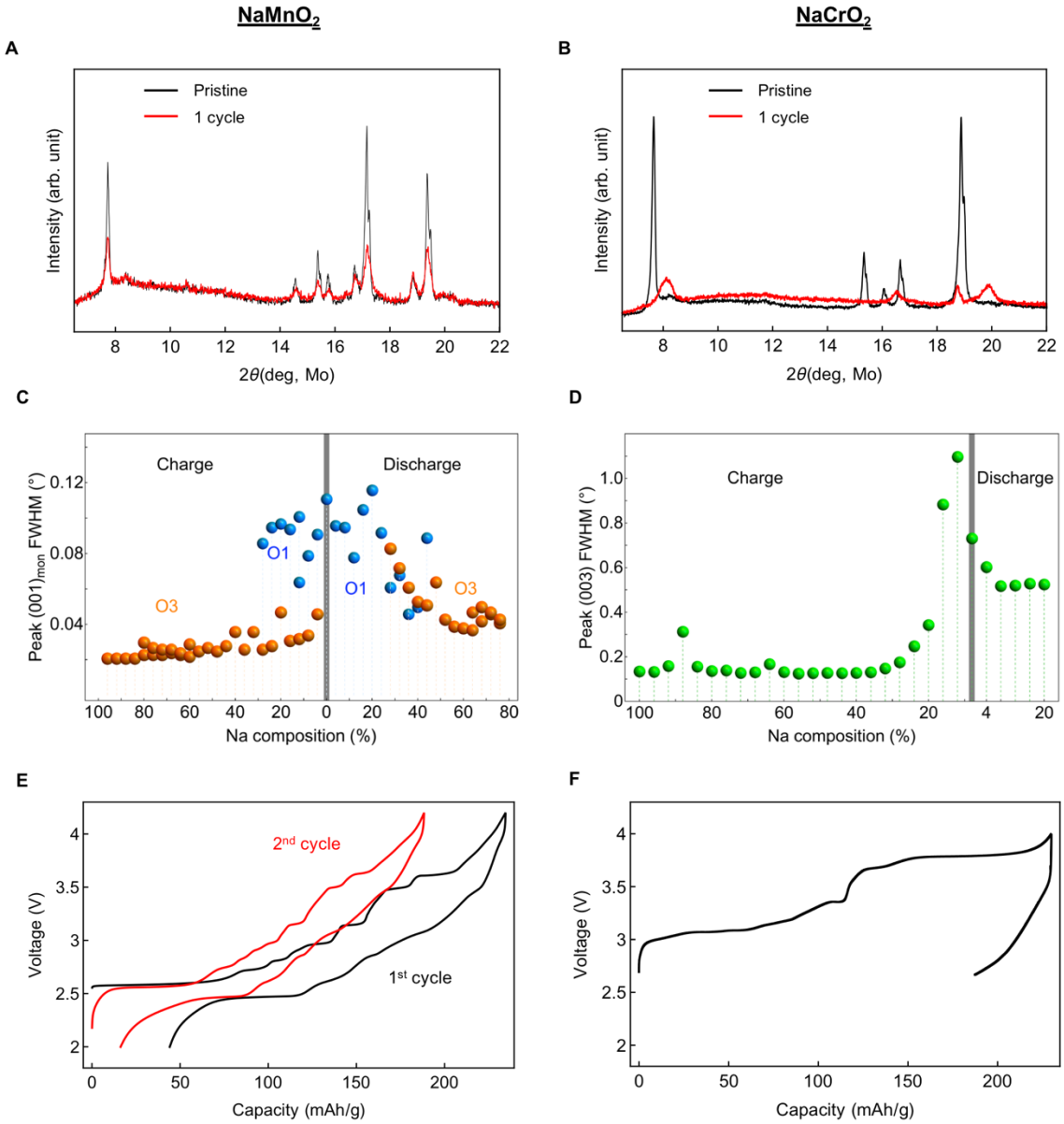

Figure S3 | Reversible evolution of $NaMnO_2$ and irreversible evolution of $NaCrO_2$. (**A**) *in-situ* XRD profiles of pristine and one cycled $NaMnO_2$. The peak positions are well matched. (**B**) *in-situ* XRD profiles of pristine and one cycled $NaCrO_2$. The peak profile after one cycle is greatly changed. (**C, D**) Evolution of the FWHM of monoclinic (001) peak for $NaMnO_2$ by *in-situ* synchrotron XRD and (003) peak for $NaCrO_2$ measured by *in-situ* lab XRD during the first cycle. (**E**) charge-discharge curves of $NaMnO_2$ in the first and second cycle from 2V to 4.2V. The charge and discharge curves are asymmetric in each cycle, but with largely reversible features from cycle to cycle. (**F**) Irreversible charge-discharge evolution of $NaCrO_2$.

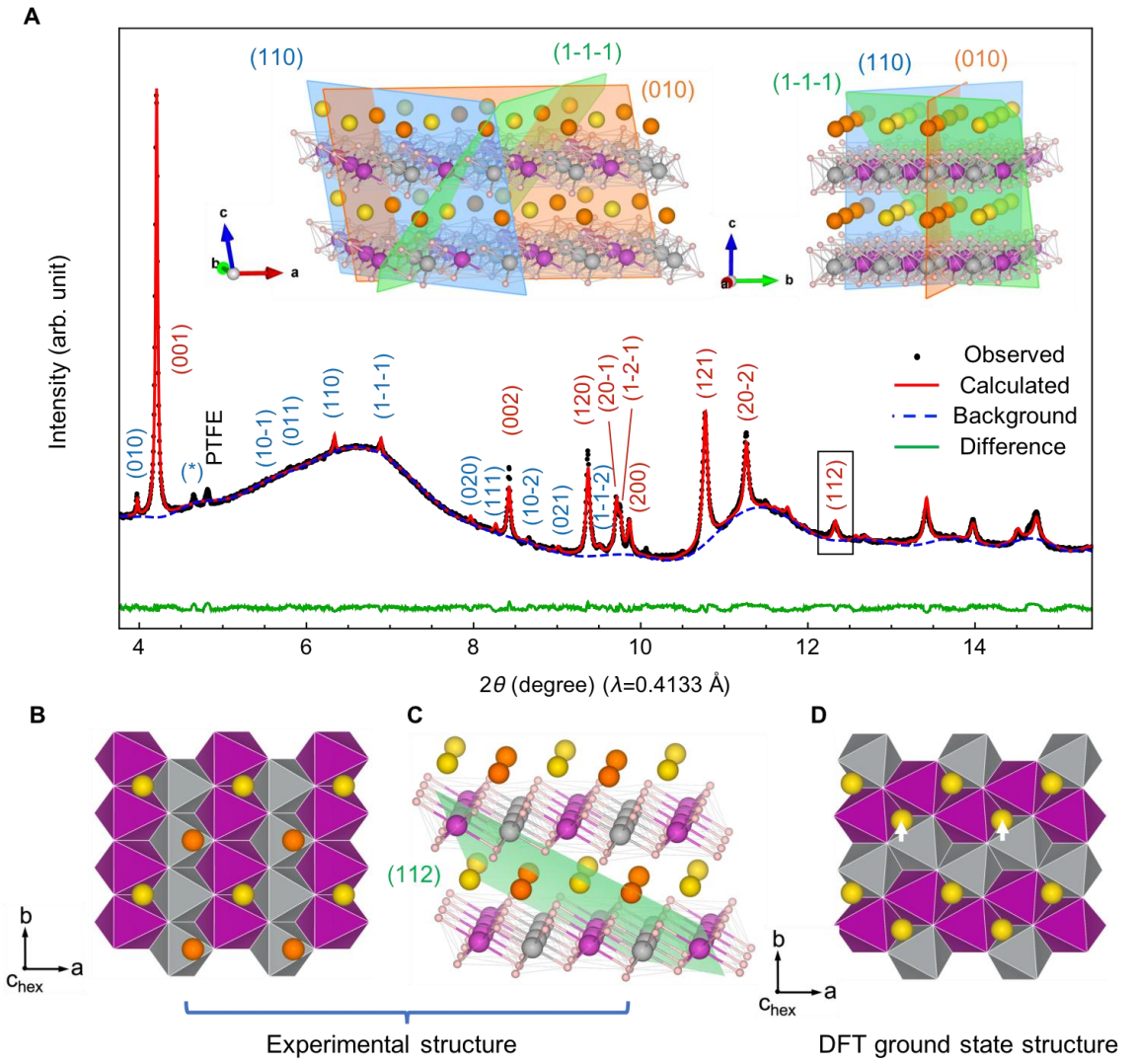

Figure S4 | Rietveld refinement of the *in-situ* SXRD for $Na_{0.5}MnO_2$ (Space group: P2/m) superstructure. (A) The SXRD refinement. The refined lattice parameter, the coordinate of ions and Na-O and Mn-O bond lengths are shown in Table S1 and S2. The hkl labels are based on the refined supercell, and the superstructure peaks are indexed in blue. Three planes, (110), (1-1-1) and (010) that contribute to the three strongest superstructure peaks, are illustrated in the two insets. (*) is at the (400) superstructure peak position of $Na_{5/8}MnO_2$[1] that does not completely disappear yet. (B) The basal MnO_2 and Na plane of the reported Na-1/2 ordering structure from SXRD experiments, also shown in Figure 3 of the Main Text. (C) The illustration of the (112) plane in the experimental structure, cutting exactly through the displaced Na sites and making itself observable in the SXRD measurement. (D) The DFT ground state of Na-1/2 ordering provided by reference 33 of the Main Text. The movement of

Na away from the displaced site breaks the (112) plane and results in the (112) peak extinguishment in the XRD refinement, leading to worse refinement.

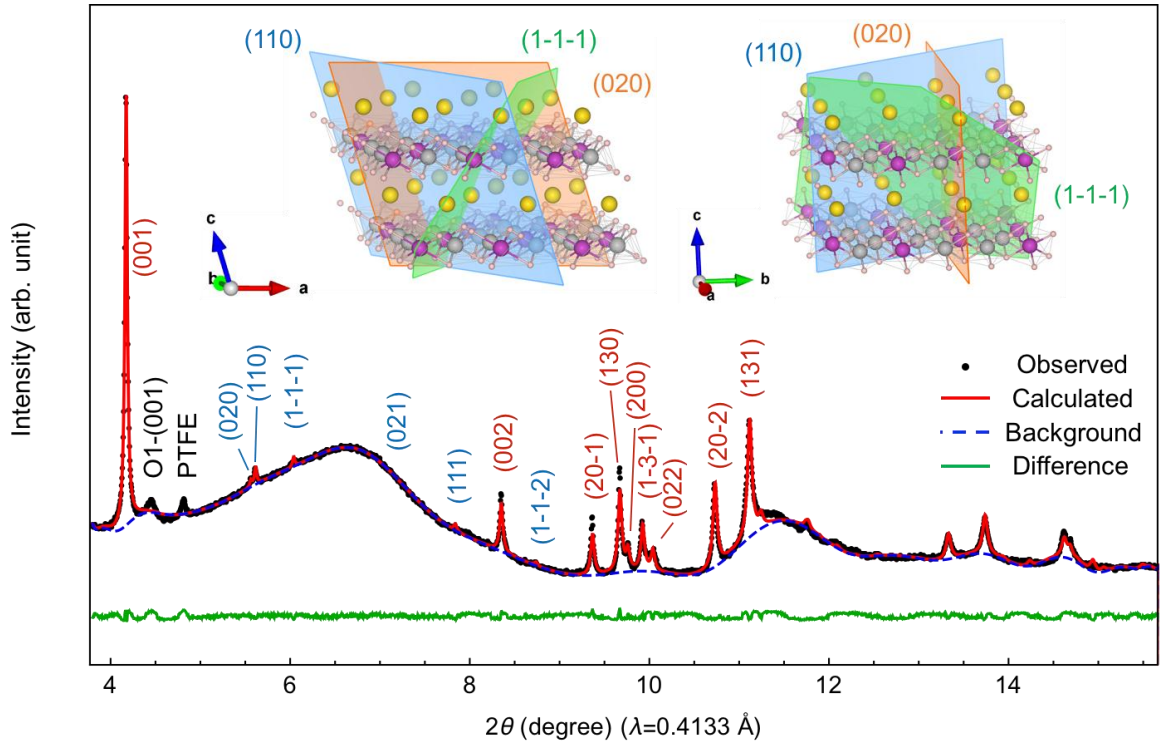

Figure S5 | Rietveld refinement of the *in-situ* SXRD for $Na_{1/3}MnO_2$ (Space group: C2/m) superstructure. The refined lattice parameter, the coordinate of ions and Na-O and Mn-O bond lengths are shown in Table S3 and S4. The hkl labels are based on the refined supercell, and the superstructure peaks are indexed in blue. Three planes, (110), (1-1-1) and (020) that contribute to the three strongest superstructure peaks, are illustrated in the two insets.

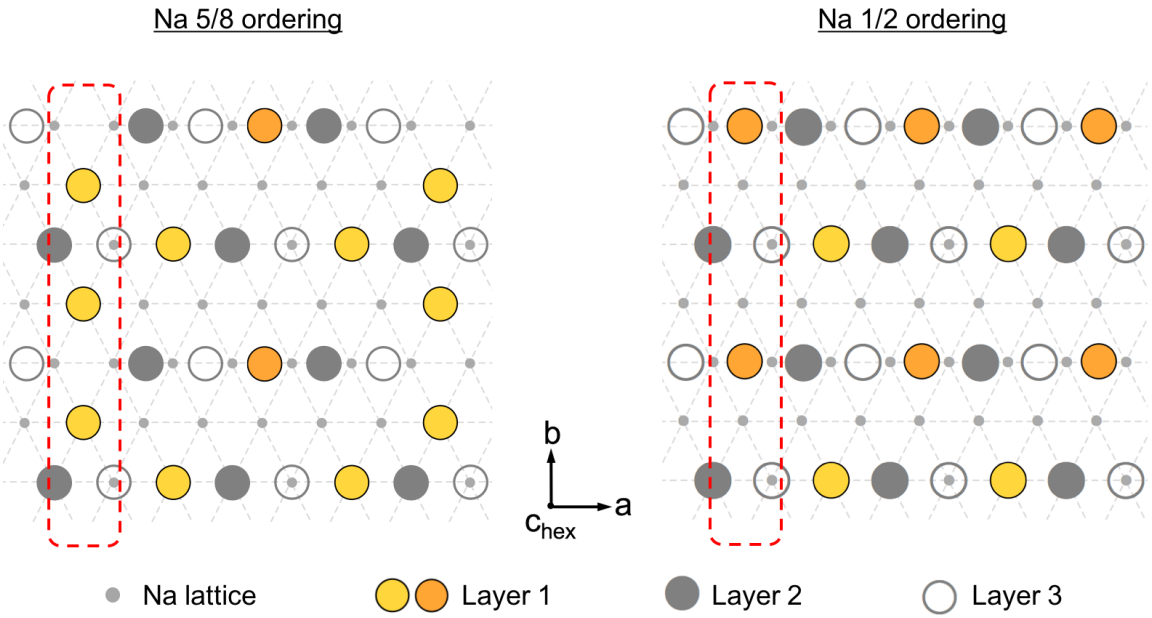

Figure S6 | Superstructure evolution from $Na_{5/8}MnO_2$ to $Na_{0.5}MnO_2$. The only full-Na row in $Na_{5/8}MnO_2$[1] evolves to a displaced half-Na row in $Na_{0.5}MnO_2$ (red dashed boxes) upon 1/8 de-intercalation of the total Na composition, while the other three rows of Na ions are at the same positions.

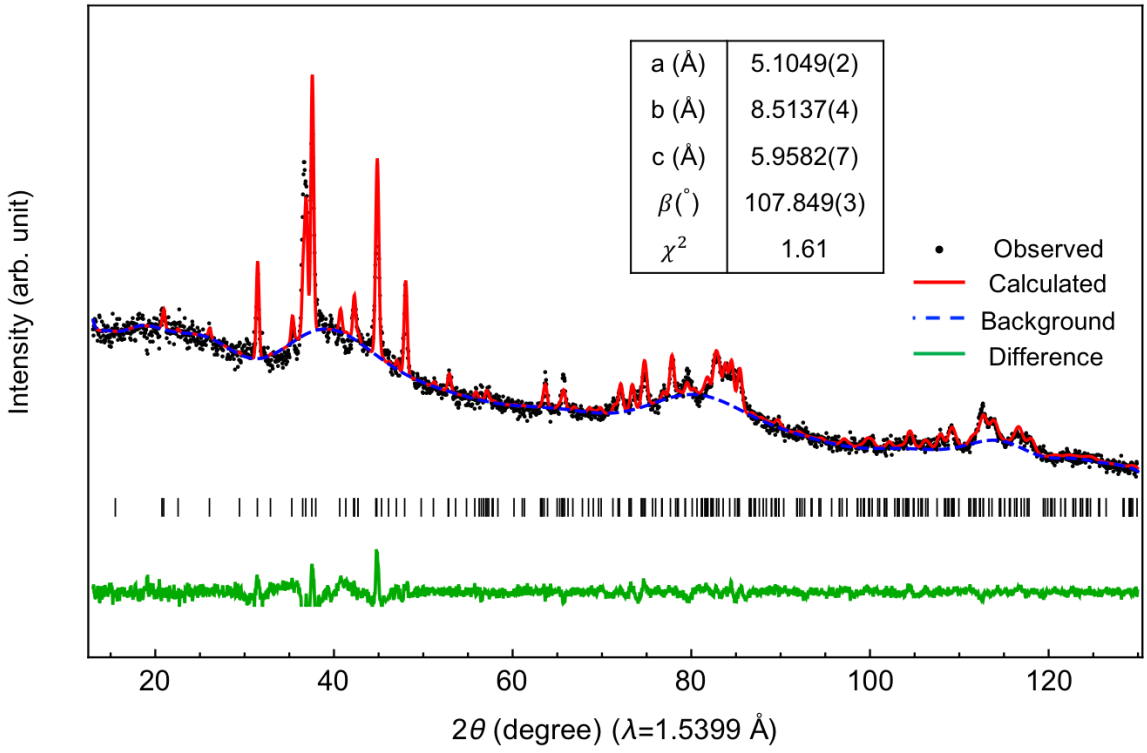

Figure S7 | Refinement of $Na_{1/3}MnO_2$ neutron diffraction pattern at room temperature. Same supercell as shown in Table. S3 for Na-1/3 XRD refinement is used. The refined lattice parameters (inset) are used as reference for simulating low-temperature magnetic peaks.

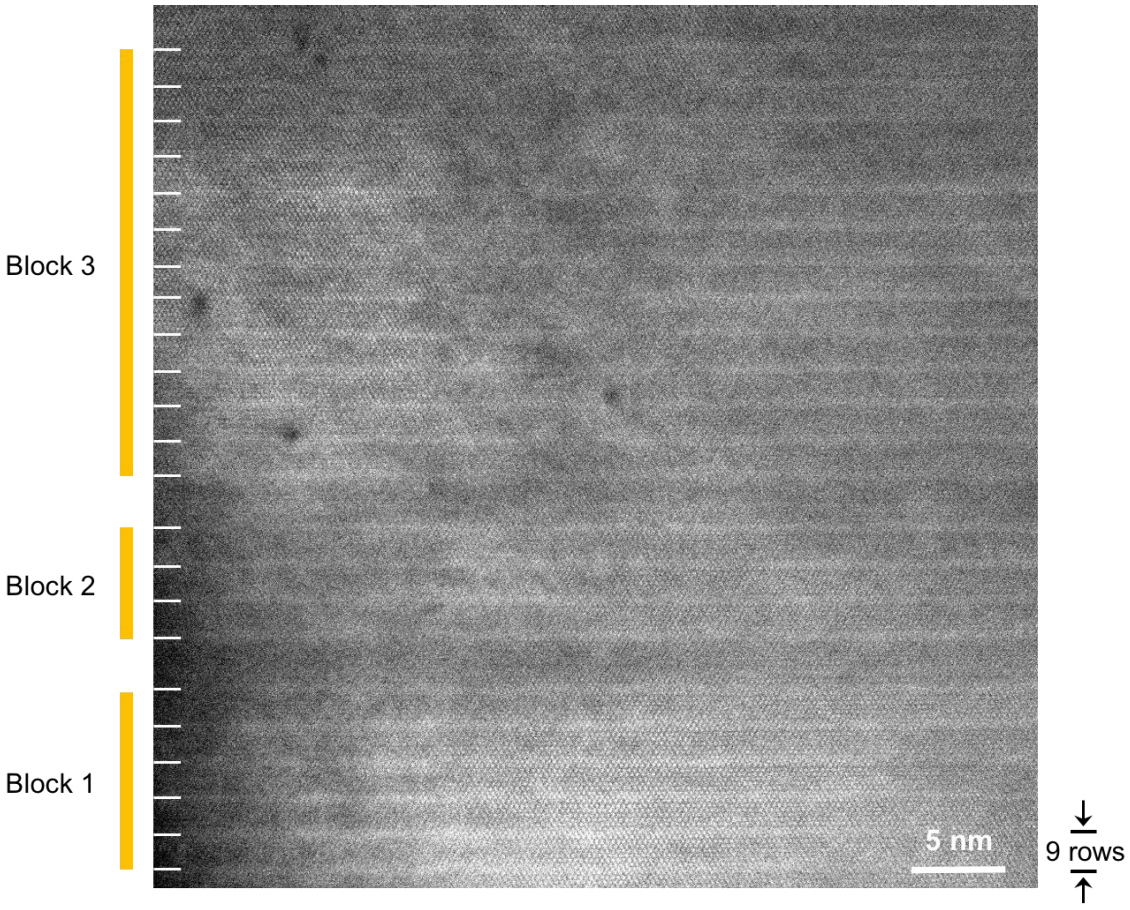

Figure S8 | Low magnification STEM image along [101] direction of $Na_{0.06}MnO_2$ at 4.0V. The distance between bright stripes are 9 rows within each block, as marked by yellow bars. White rods indicate the center of each Na stripe.

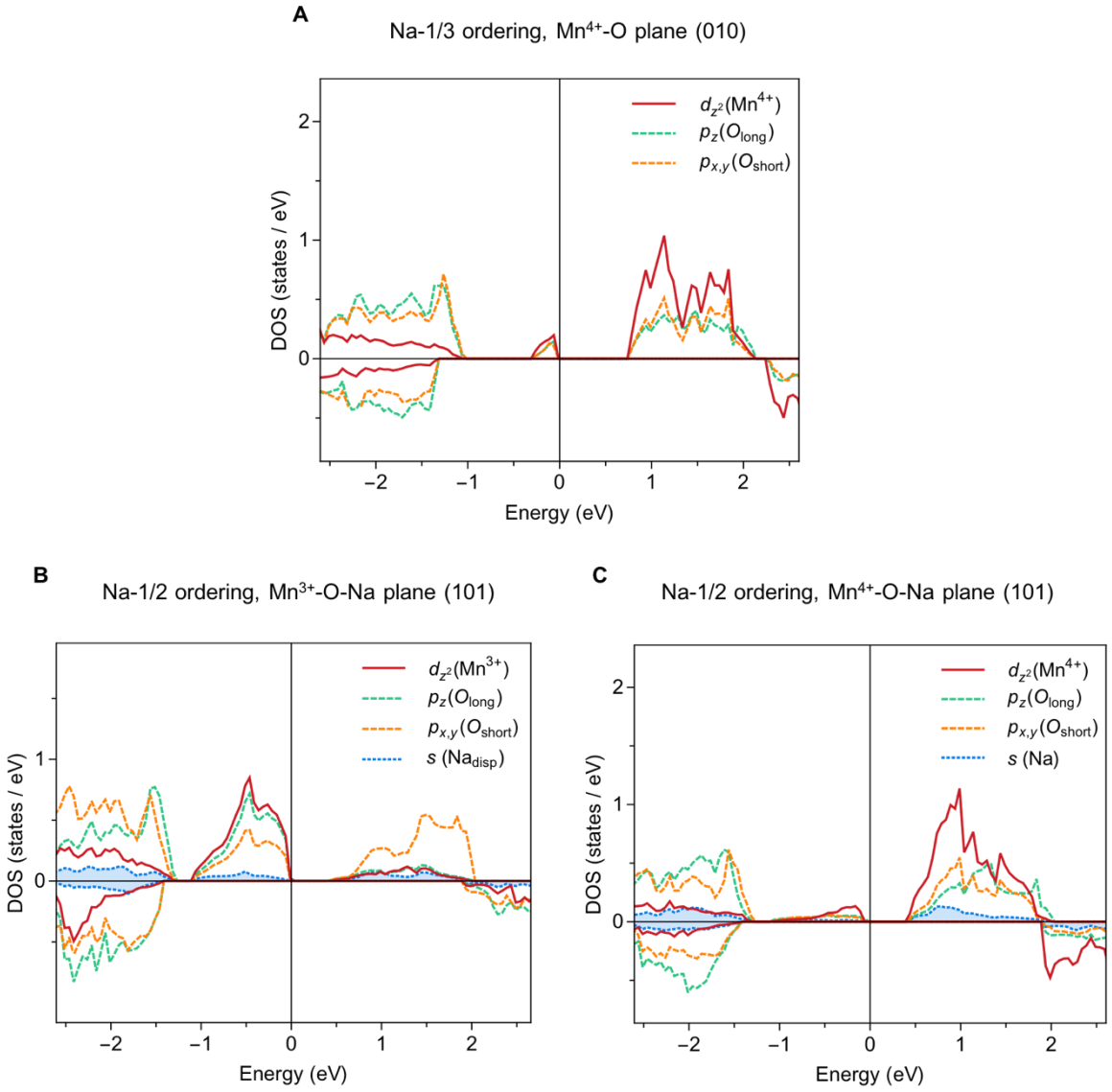

Figure S9 | DOS of the d_{z^2} orbital of Mn, the p orbitals of O and the s orbital of Na in the super-plane of Na -1/2 and Na -1/3 orderings. The DOS calculation of the Mn^{3+} super-plane of Na-1/3 ordering is in Fig. 7A of the Main Text. The definition of x, y, and z is also following Fig. 7A, with z being the JT long axis. Note that Na is absent in the Mn^{4+} super-plane for Na-1/3 ordering. The magnitude of DOS is square root of the calculated value. The DOS peaks corresponding to s induced pd hybridization below the Fermi level in the Mn^{4+} super-plane is more than an order of magnitude lower than in the Mn^{3+} super-planes, showing that such hybridization is strongly coupled with JT active Mn^{3+}.

O'3-$Na_{1/2}MnO_2$	a[Å]	b[Å]	c[Å]	β[deg]	Space group
	4.9621(5)	5.9485(8)	5.8088(9)	104.485(8)	P/2m
#	Atom	Site	x	y	z	Beq.
1	Mn1(4+)	1d	0	0	0.5	5.1569(8)
2	Mn2(3+)	2l	0.5	0.7387(0)	0.5	4.9511(3)
3	Mn3(4+)	1e	0	0.5	0.5	4.4413(5)
4	O1	4o	0.1953(0)	0.7298(0)	0.6770(0)	4.2525(9)
5	O2	2n	0.7235(0)	0.5	0.6652(3)	2.7089(1)
6	O3	2m	0.6987(1)	0	0.6421(0)	3.3698(7)
7	$Na1_{disp}$	1f	0.5	0.5	0	0
8	Na2	1a	0	0	0	17.9586(4)
Agreement factors:		Rexp=1.48%	Rwp=3.51%	Rp=2.43%		

Table S1 | The SXRD refinement result of $Na_{1/2}MnO_2$ (space group P2/m). Beq. is related to the isotropic thermal parameter. The ion coordinates are only allowed for less than 2% deviation in the refinement from the DFT relaxed input positions.

Atom	Bond	Bond Length(Å)	Multiplicity
Mn1	Mn1-O1	2.0202(1)	4
	Mn1-O3	1.8798(6)	2
Mn2	Mn2-O1	2.0306(9)	2
	Mn2-O2	1.9272(9)	2
	Mn2-O3	1.9137(6)	2
Mn3	Mn3-O1	1.8347(9)	4
	Mn3-O2	1.8222(2)	2
$Na1_{disp}$	Na1-O1	2.5011(7)	4

	Na1-O2	2.4970(0)	2
Na2	Na2-O1	2.8200(4)	4
	Na2-O3	2.2366(1)	2

Table S2 | Mn-O and Na-O distance calculated from the $Na_{1/2}MnO_2$ structure after Rietveld refinement. Refinement indicates two long Mn-O bonds and four short bonds for Mn2, which is also the JT active Mn^{3+} according to DFT calculation.

O'3-$Na_{1/3}MnO_2$	a[Å]	b[Å]	c[Å]	β[deg]	Space group
	5.0610(2)	8.4482(5)	5.9127(5)	107.852(3)	C/2m

#	Atom	Site	x	y	z	Beq.
1	Mn1(3+)	2a	0	0	0	0
2	Mn2(4+)	4g	0.5	0.1618(1)	0	5.922
3	O1	4i	0.6867(0)	0	0.1711(0)	14.38
4	O2	8j	0.7568(0)	0.1726(0)	0.8324(2)	0.6848
5	Na1	2d	0.5	0	0.5	5.422
Agreement factors:		Rexp=1.46%	Rwp=3.48%	Rp=2.44%		

Table S3 | The SXRD refinement result of $Na_{1/3}MnO_2$ (space group C2/m). Beq. is related to the isotropic thermal parameter. The ion coordinates are only allowed for less than 2% deviation in the refinement from the DFT relaxed input positions.

Atom	Bond	Bond Length(Å)	Multiplicity
Mn1	Mn1-O1	2.1263(2)	2
	Mn1-O2	1.9685(7)	4
Mn2	Mn2-O1	1.7885(5)	2

	Mn2-O2	1.8624(9)	2
	Mn2-O2	1.9251(2)	2
Na1	Na1-O1	2.4085(9)	2
	Na1-O2	2.4723(1)	4

Table S4 | Mn-O and Na-O distance calculated from the $Na_{1/3}MnO_2$ structure after Rietveld refinement. Refinement indicates two long Mn-O bonds and four short bonds for Mn2, which is also the JT active Mn^{3+} according to DFT calculation.

1 X. Li, X. Ma, D. Su, L. Liu, R. Chisnell, S. P. Ong, H. Chen, A. Toumar, J. Idrobo, Y. Lei, J. Bai, F. Wang, J. W. Lynn, Y. S. Lee and G. Ceder, *Nat. Mater.*, 2014, **13**, 586–592.